2016 International Conference on Distributed Computing in Sensor Systems

Error Bounds for Localization with Noise Diversity

Duc V. Le, Jacob W. Kamminga, Hans Scholten, and Paul J.M. Havinga
Pervasive Systems Group, Department of Computer Science
Faculty of Electrical Engineering, Mathematics and Computer Science
University of Twente, Drienerlolaan 5, 7522 NB Enschede, The Netherlands
Email: {v.d.le, j.w.kamminga, hans.scholten, p.j.m.havinga}@utwente.nl

***Abstract*—In the context of acoustic monitoring, the location of a sound source can be passively estimated by exploiting time-of-arrival and time-difference-of-arrival measurements. To evaluate the fundamental hardness of a location estimator, the Cramer-Rao bound (CRB) has been used by many researchers. The CRB is computed by inverting the Fisher Information Matrix (FIM), which measures the amount of information carried by given distance measurements. The measurements are commonly expressed as actual distances plus white noise. However, the measurements do include extra noise types caused by time synchronization, acoustic sensing latency, and signal-to-noise ratio. Such noise can significantly affect the performance and depend highly on the sensing platforms such as Android smartphones. In this paper, we first remodel the acoustic-based distance measurements considering such additive errors. Then, we derive a new FIM with the new statistical ranging error models. As a result, we obtain new CRBs for both non-cooperative and cooperative localization schemes that provide better insight into the causality of the uncertainties. Theoretical analysis also proves that the proposed CRBs for localization become the old CRBs when the additional errors are ignored, which gives a robust check for the new CRBs. Thus, the new CRBs can serve as a benchmark for localization estimators with both new and old measurement models. The new CRBs also indicate that there is room to improve current localization schemes; however, it is a daunting challenge.**

***Keywords*-sound localization; Cramer-Rao bound; time of arrivals; time difference of arrivals; smartphone diversity; noise diversity**

I. Introduction

That smartphones with onboard sensors are present everywhere and wirelessly connected promises a low-cost sensing system for sound source localization applications. However, sound source localization with current smartphones is a daunting challenge, especially in indoor environments and areas blocked by buildings and trees. Common approaches use either infrastructure-based anchors [1] or less non-deterministic smartphones such as iPhones [2], [3]. Nevertheless, more than 80% smartphone subscriptions are Android devices that have considerable acoustic uncertainties of the time synchronization, processing latency, and the signal-to-noise ratio (SNR). For example, our experiments with 16 Nexus 7 tablets revealed the standard deviations of audio latency approximate to 7 ms and of time synchronization about 8 ms. That means the error of ranging can add up to $(7 + 8)$ ms$\times 0.34029$ m/ms ≈ 5 m, where 0.34029 m/ms is the speed of sound. Meanwhile, the sum of such latencies is approximate $1\ ms$ for iPhones and a few microseconds for dedicated sensor devices in wireless sensor networks [4]. Our experiments also showed that the SNR added a noise approximate 1 m to the estimated distances. This issue deters location-based acoustic sensing applications with commercial smartphones from being deployed on a large scale. The theoretical bound for acoustic localization that will be presented in this paper can serve as a tool to aid designing a localization system.

In general, either the Bayesian Bound (BB) [5], the Geometrical Dilution of Precision (GDOP) [6], or the Cramer-Rao bound (CRB) [7] can be used as the error bound for localization estimators. As today life is dominated by smartphones integrated navigation systems, there is frequently an abundance of them in public events that can be used as anchors. Thus, the acoustic source localization problem is close to unbiased. On the other hand, the CRB is the most suitable tool for unbiased estimators, especially when the tolerable noise and geometrical setup are considered like pointed out in [5] and [6], which respectively compare the BB and the GDOP to the CRB.

There exist articles studying the CRB for different noise models including the distance-independent variance model [8], [9] and the distance-dependent variance model [10]. However, through the experiments with Android devices, we noticed that practical noises consist of three main terms: the variances of time-of-arrival (TOA) and time-difference-of-arrival (TDOA) increasing with distance from the source emitter due to the variance of the SNR; the variance of the acoustic latency; and the variance of the time synchronization. Since these additive noises are very small in dedicated acoustic sensing platforms in the conventional systems, they have not been simultaneously taken into account when deriving the CRB for localization in previous work.

Therefore, in this paper, we derive the CRBs for localization with regard to such additive errors, which can be closely modeled as a mix of Gaussian distribution, namely the multivariate Gaussian mixture model. The derivation leads to new CRBs that provide better insight into the effects of the additive noises. In particular, we first introduce an application we built to measure and analyze the nuisance (unknown) parameters of the additive errors: the variances

2325-2944/16 $31.00 © 2016 IEEE
DOI 10.1109/DCOSS.2016.18

of clock synchronization, acoustical sensing latency, and signal-to-noise ratio. Next, we propose new statistical models for the TOA and TDOA. Considering the realistically proposed errors in ranging, we derive the new CRBs for both TOA and TDOA. The numerical examples based on the experimental parameters show that the localization accuracy for each position heavily depends on the geometric of all anchors in the network rather than the acoustic latency. In addition, the new CRBs confirm that the localization performance can be improved by increasing the number of smartphones.

The remainder of this paper is organized as follows. After describing the related work in Section II, we define the problem in Section III. Section IV proposes new acoustic-based distance models for the TOA and TDOA. Section V describes the localization models with the assistance of anchors with regard to non-cooperative and cooperative localization. The derivation of CRB for anchored localization is presented in Section VI step by step. Finally, we conclude this work with Section VII.

II. Related Work

In fact, the Cramér-Rao bound has been widely studied as the aid of design to estimate the error bounds for localization estimators [7]–[17]. In [8], [9], the expression of the CRB is derived for cooperative localization with the TOA measurements. The CRB expressed by [8], [9] will be referred as the old CRB in our work since they assume that the TOA measurement uncertainties are independent of the distance between emitters and receivers. While this assumption is valid in traditional WSNs with numerous sensors and anchors, Dulman et. al. showed that the old CRB fails to capture the geometric characteristics of certain anchors setup in [14], [16] through the simulation examples. Therefore, they proposed to optimize the anchor placements in order to lessen impacts of geometric setup. This proposal indeed overlaps the well-known problem in localization, the anchor placement problems [18]–[20]. Conversely, Toa Jia and Michael Bueher grasped the geometry effects by deriving the CRB for TOA based on the distance-dependent variance model for range estimation noise [10]. The derivation leads to the better CRB, which gives a lower bound and provides better insight into the impacts of the anchor placements on localization accuracy. In [11], the CRBs for non-line-of-sign (NLOS) environments are proposed to overwhelm the inaccuracy of the old CRBs when the geometric setup is not ideal.

Besides the CRB, BB and GDOP also serve as the benchmarks of localization estimators. [5] studies that the BB equals the CRB when the observed error is Gaussian. The GDOP is derived from the CRB by simplifying the assumption of the ranging error models, in which variances of all distance estimates are equal [6], [8]. This assumption is not perfectly valid in localization with human-oriented devices such as smartphones, since the uncertainties are diverse. On the other hand, it is common to see plenty of people carrying smartphones at public places that can play as anchors for localization, especially during events and festivals. This makes the CRB still valid for localization estimators if the tolerable noise and geometrical setup are considered. Using the CRB also allows using the full distance information to estimate better the error bound for unbiased estimators. Therefore, we address the CRB approach in this paper.

III. Problem Statement

Without loss of generality, we consider a network comprising a set S of n acoustic emitters with unknown location information, namely source nodes, and a set A of m acoustic sensor devices such as smartphones with known location information, namely anchor nodes. We assume that the size of the nodes is small enough to be treated as a point on a 2D localization map, which has the coordinate $x = (x, y)^T \in R^2$. Each source node generates a limited-power acoustic signal that can be used to estimate the distance to the receivers. Let N_k denote the set of nodes in the range of the k^{th} node. Note that a source node can be either natural or synthesized. N_k might consist of not only anchor nodes but also source nodes that can receive the acoustic signal from the k^{th} node.

Given the ranging measurements from the k^{th} node to its neighboring nodes N_k, the problem is to find the error bound for the estimated locations of the k^{th} node with respect to the uncertainties included in the measurements.

Since most modern smartphones possess some accurate positioning systems, we will focus on the lower error bounds for anchored localization in this work. For anchor-free localization, the standard CRB analysis fails due to the Fisher Information Matrix (FIM) is singular [21], [22]. Nevertheless, [9] interprets geometry on a modified CRB and derives some properties of it. Therefore, the lower bound error for anchor-free localization is straightforward.

IV. Statistical Models

Most previous work assume that the variance is constant for all nodes and independent from the distance [8], [9]. This is not absolutely correct since the noise of an acoustic signal is distance-related, proved by [23], [24], the bound for distance estimation is a function inversely proportional to SNR. [10] corrects this by modelling the variance as $K_e d_{ki}^{\beta}$ where K_e is a proportionality constant to capture the combined physical layer effect on the distance estimate and β is the path loss exponent. This model is for simplicity and can be more realistic. However, it does not affect our derivations since the variance of noise by this model is also inversely proportional to the SNR.

The models we proposed in this paper specifically target acoustic-based range measurements that include the afore-

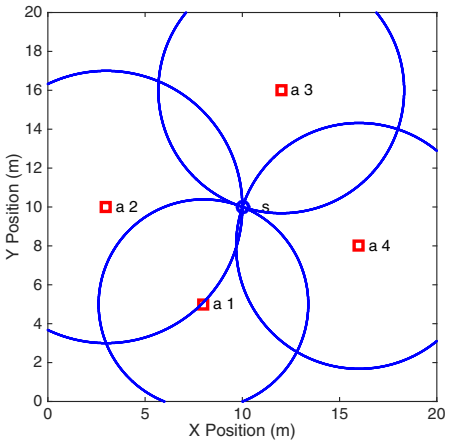

Figure 1. TOA model with circles to estimate unknown location of sound source s given the location of receivers a.

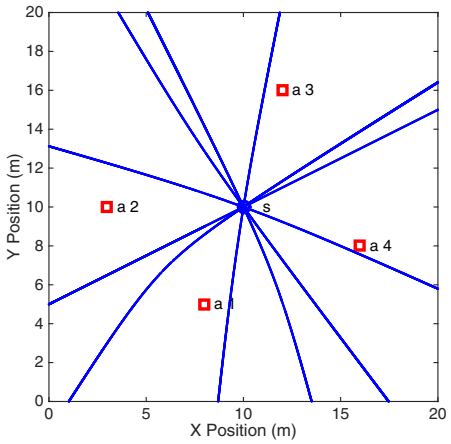

Figure 2. TDOA model with hyperbolic lines to estimate the location of the source s given the location of receivers a.

mentioned major errors. These errors lead to new statistical models of the TOA and TDOA measurements.

A. Time of Arrival (TOA)

If the time of signal emission is known, the distance can be inferred directly by TOA. Without loss of generality, we consider the TOA distance from an arbitrary emitter $k,\ k \in S$, to an arbitrary neighbour receiver $i,\ i \in N_k$. The true distance from the k^{th} node to the i^{th} node, of which actual 2D positions are respectively $(x_k, y_k)^T$ and $(x_i, y_i)^T$, is denoted by d_{ki}. The source emitter location can be estimated by the intersections of circles illustrated in Fig. 1, of which radiuses are the distances $\{d_{ki},\ i \in N_k\}$.

Definition 1: (TOA) Let δ_{ki} denote the TOA distance measurement and η_{ki} denote the corresponding noise, then distance model based on TOA is given by

$$\Delta = \{\delta_{ki} = d_{ki} + \eta_{ki} | k \in S, i \in N_k\}, \tag{1}$$

where

$$d_{ki} = \sqrt{(x_i - x_k)^2 + (y_i - y_k)^2} \tag{2}$$

is the actual distance.

Our experimental results show that the noise is close to a Gaussian random variable with zero mean and some variance, $\eta_{ki} \sim N(0, \sigma_{ki}^2)$. As being pointed out, the noise is mainly contains the variances of the decay of signal propagation $K_e d_{ki}^{\beta}$, the acoustic sensing latency ξ_i^2 and the time synchronisation errors ζ^2.

Lemma 1: (TOA Noise Model) Let δ_{ki} be influenced by noises that have Gaussian distribution: $N(0, K_e d_{ki}^{\beta})$, $N(0, \xi_i^2)$ and $N(0, \zeta^2)$. Then the distribution of η_{ki} is also Gaussian:

$$\eta_{ki} \sim N(0, \sigma_{ki}^2), \tag{3}$$

where

$$\sigma_{ki}^2 = K_e d_{ki}^{\beta} + \xi_i^2 + \zeta^2. \tag{4}$$

Proof: Since the partial noise distributions are assumed to be normally distributed independent variables:

$$\begin{aligned} X_1 &\sim N(0, K_e d_{ki}^{\beta}) \\ X_2 &\sim N(0, \xi_i^2) \\ X_3 &\sim N(0, \zeta^2), \end{aligned}$$

then their sum $\eta_{ki} = X_1 + X_2 + X_3$ is also normally distributed, $\eta_{ki} \sim N(0 + 0 + 0, K_e d_{ki}^{\beta} + \xi_i^2 + \zeta^2)$. ■

B. Time Different of Arrival (TDOA)

If the emission time of the k^{th} source emitter is unavailable, then the TDOA technique is frequently used. The actual distance from the k^{th} source node to the i^{th} receiver cannot be computed directly like TOA. It has to be paired with the distance from the same k^{th} emitter to another j^{th} receiver in the neighborhood, $j \neq i$ and $i, j \in N_k$. In fact, the actual TDOA distance is $d_{kij} = d_{kj} - d_{ki}$.

Note that each d_{kij} corresponds to a position $(x, y)^T$ along a hyperbola that goes through the k^{th} source node between the i^{th} and j^{th} nodes. Finding the intersections of such hyperbolic lines will give the estimated position of the k^{th} source node, see Fig. 2.

Definition 2: (TDOA) Let δ_{kij} denote the TDOA distance measurement and η_{kij} denote the corresponding noise, then the distance model based on TDOA is

$$\Delta = \{\delta_{kij} = d_{kij} + \eta_{kij} \mid k \in S,\ i, j \in N_k,\ j > i\}, \tag{5}$$

where

$$d_{kij} = d_{kj} - d_{ki}. \tag{6}$$

Lemma 2: (TDOA Noise Model) Let $\eta_{ki} \sim \mathcal{N}(0, \sigma_{ki}^2)$ and $\eta_{kj} \sim \mathcal{N}(0, \sigma_{kj}^2)$. Then the distribution of η_{kij} is also Gaussian:

$$\eta_{kij} \sim \mathcal{N}(0, \sigma_{kij}^2), \tag{7}$$

where

$$\sigma_{kij}^2 = \sigma_{ki}^2 + \sigma_{kj}^2 = K_e(d_{ki}^\beta + d_{kj}^\beta) + \xi_i^2 + \xi_j^2 + 2\zeta^2. \quad (8)$$

Proof: Since the variance model of the TOA range measurements are normally distributed random variables,

$$X_1 \sim N(0, \sigma_{ki}^2)$$
$$X_2 \sim N(0, \sigma_{kj}^2),$$

then their subtraction $\eta_{kij} = X_2 - X_1$ is also normally distributed, $\eta_{kij} \sim N(0-0, \sigma_{ki}^2 + \sigma_{kj}^2)$. ■

We remark that for the TDOA model, the measurement set of each source node consists of $|N_k|(|N_k|-1)/2$ possible TDOA measurements [25], illustrated as the number of hyperbolic lines in Fig. 2. Meanwhile, the measurement set of each source node with TOA model contains only $|N_k|$ distinguished TOA measurements, illustrated as the number of circles in Fig. 1.

V. Anchored Localization Models

Within anchored localization, the localization problem is categorised into non-cooperative localization and cooperative localization. Non-cooperative localization estimates the unknown locations, given location information of anchor nodes only. Conversely, cooperative localization uses not only location information given by anchor nodes, but also estimated location information of other source nodes. This categorization leads to different models for non-cooperative and cooperative localizations.

In non-cooperative localization, all the source nodes act as emitters only. In other words, the locations of source nodes can only be estimated using location information of anchor nodes. The common application of this model is localizing natural acoustic sources, for instance, where a car is sounding the horn or a glass is broken.

Definition 3: (Non-cooperative Localization) If $N_k \subseteq A$, $\forall k \in S$ and $|A| \geqslant 3$ (in 2D space), then it is possible to estimate the absolute coordinates of each source node $X_S = \{(x_k, y_k)^T \mid k \in S\}$ given observations Δ and known location information of anchor nodes in N_k.

On the other hand, if the source nodes can simultaneously transmit and receive acoustic signals, they can provide their location information to their neighbors to obtain better estimates. In other words, the location of a sound node can be estimated by not only the known locations of anchors but also the estimated locations of other sound nodes. This technique is called cooperative localization. A common application of cooperative localization is localizing devices that can emit synthesized sounds.

Definition 4: (Cooperative Localization) If $N_k \nsubseteq A$, $\forall k \in S$ and $|A| \geqslant 3$ (in 2D space), it is possible to estimate the absolute coordinates of each source node $X_S = \{(x_k, y_k)^T \mid k \in S\}$, given the observations Δ, the known location of anchor nodes, and estimated location of source nodes in N_k.

VI. CRB for Anchored Localization

The FIM has been derived to compute the CRB by [8]–[10]; however, we derive the FIM again in this work since the uncertainty models have been modified. Let θ denote the unknown parameters that need to be estimated, and $\theta \in \Theta$, where Θ is the parameter space. We have

$$\Theta = \{\theta_k,\ k \in S\}. \quad (9)$$

In our localization problem, θ_k is the estimated coordinates of the k^{th} node, $\theta_k = (\hat{x}_k, \hat{y}_k)$. Let the probability function of δ, which is also the likelihood function of Θ, be the function $f(\delta|\theta)$. If $\log f(\delta|\Theta)$ is twice differentiable with respect to Θ, the FIM is computed by

$$J = -E\left[\frac{\partial^2 \log f(\delta|\Theta)}{\partial \theta_k^2}\Big|\Theta\right] \quad (10)$$

Suppose that the distance measurements are normally distributed around the actual distance, we derive the FIM for the TOA and TDOA.

A. FIM for TOA

The conditional probability density function (pdf) of δ given Θ:

$$f(\delta|\Theta) = \prod_{k\in S} f(\delta|\theta_k) = \prod_{\substack{k\in S \\ i\in N_k}} \frac{1}{\sqrt{2\pi}\sigma_{ki}} e^{-\frac{(\delta - d_{ki})^2}{2\sigma_{ki}^2}} \quad (11)$$

where d_{ki} and σ_{ki} are given by (2) and (4) respectively. To derive the FIM, we define $L(\delta|\theta_k) = \log f(\delta|\theta_k)$ as the log-likelihood function, and

$$\begin{aligned} L(\delta|\theta_k) = &-\log\sqrt{2\pi} \\ &- \frac{1}{2}\log(K_e d_{ki}^\beta + \xi_i^2 + \zeta^2) \\ &- \frac{(\delta - d_{ki})^2}{2(K_e d_{ki}^\beta + \xi_i^2 + \zeta^2)}. \end{aligned} \quad (12)$$

Partially derivating $L(\delta|\theta_k)$ twice, we obtain the FIM elements for the non-cooperative anchored localization and cooperative localization given the TOA measurements. For simplification, we express the FIM as a function of angles between nodes. For example, the angles between the k^{th} node and the i node is defined as:

$$\begin{aligned} \cos\alpha_{ki} &= \frac{x_i - x_k}{d_{ki}}, \\ \sin\alpha_{ki} &= \frac{y_i - y_k}{d_{ki}}. \end{aligned} \quad (13)$$

Theorem 1: (FIM for Non-cooperative TOA) Every arbitrary k^{th} source node has its own FIM denoted by $J_{2\times 2}$, of

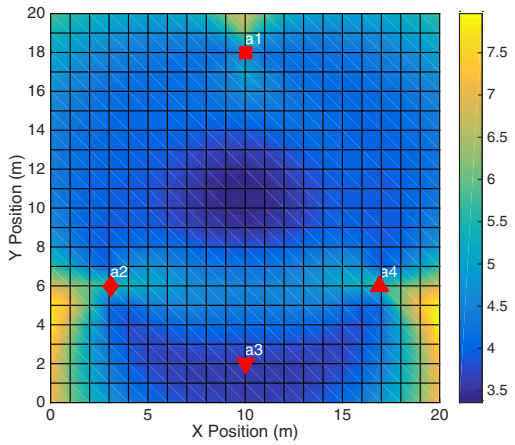

Figure 3. New CRB for TOA non-cooperative localization with four different kinds of anchors. Color bar on the right indicates error bound in meters.

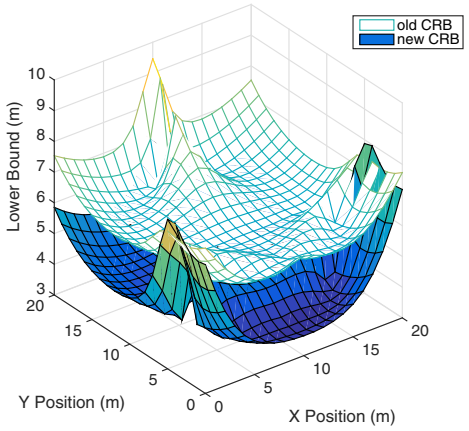

Figure 4. Old CRB vs. new CRB for TOA non-cooperative localization with the average standard deviation of noises is 5.64 meters.

which elements are

$$J_{1,1} = \sum_{i \in N_k \bigcap A} \frac{\omega_{ki} \cos^2 \alpha_{ki}}{\sigma_{ki}^2},$$
$$J_{2,2} = \sum_{i \in N_k \bigcap A} \frac{\omega_{ki} \sin^2 \alpha_{ki}}{\sigma_{ki}^2}, \quad (14)$$
$$J_{1,2} = J_{2,1} = \sum_{i \in N_k \bigcap A} \frac{\omega_{ki} \cos \alpha_{ki} \sin \alpha_{ki}}{\sigma_{ki}^2},$$

where

$$\omega_{ki} = 1 + \frac{\beta^2 K_e^2 d_{ki}^{2\beta-2}}{2\sigma_{ki}^2} \quad (15)$$

is referred to as the scaling weight, which is always equal to 1 in the old CRBs [8], [9].

Proof: From (12) we define the following two terms

$$U = -\frac{1}{2} \log(K_e d_{ki}^{\beta} + \xi_i^2 + \zeta^2), \quad (16)$$
$$V = -\frac{(\delta - d_{ki})^2}{2(K_e d_{ki}^{\beta} + \xi_i^2 + \zeta^2)}. \quad (17)$$

Therefore, we have

$$E\left[\frac{\partial^2 L(\delta|\theta_k)}{\partial x_k^2}\right] = E\left[\frac{\partial^2 U}{\partial x_k^2}\right] + E\left[\frac{\partial^2 V}{\partial x_k^2}\right].$$

Through steps of partial derivatives, we obtain

$$E\left[\frac{\partial^2 L(\delta|\theta_k)}{\partial x_k^2}\right] = -\frac{\cos^2 \alpha_{ki}}{\sigma_{ki}^2}\left(1 + \frac{\beta^2 K_e^2 d_{ki}^{2\beta-2}}{2\sigma_{ki}^2}\right).$$

Analogously, we have other entries of J. ■

By definition, the CRB for the localization error of the k^{th} node can be described by the sum of the trace of the inverse FIM matrix denoted by J^{-1},

$$E[(\hat{x}_k - x_k)^2 + (\hat{y}_k - y_k)^2] \geqslant J_{1,1}^{-1} + J_{2,2}^{-1}. \quad (18)$$

In order to present the numerical results of our derived CRB, we consider an area of 20 m $\times$ 20 m with four anchors asymmetrically placed at coordinates $x_{a1} = (10, 18)^T$, $x_{a2} = (3, 6)^T$, $x_{a3} = (10, 2)^T$ and $x_{a4} = (17, 6)^T$, (see Fig. 3). These anchors represent for four different brand smartphones that cause different ranging errors. We set $\xi_1 \sim N(3.5, 0.1)$, $\xi_2 \sim N(2.2, 0.1)$, $\xi_3 \sim N(13, 0.1)$, and $\xi_4 \sim N(1.8, 0.1)$ that are close to our measurements of Motorola G, LG G2, Nexus 7, and Samsung Galaxy Note II, respectively.

For simplicity, we assume that K_e and β are constant, particularly $K_e = 0.004$ m^{-1} and $\beta = 3$. Note that we put more value on K_e and β to emphasise the dependence on distance. Since the average distance between two nodes in the area is 8 m, the standard deviation of noise due to signal propagation is approximate $\sqrt{0.004\ m^{-1} \times 8^3\ m^3} \approx 1.4$ m, which somewhat exaggerates our real measurement (1 m). The aim is to have a better visualization of the discrepancy between the old and new CRBs. Since localization performance with the same anchor placement and settings varies with the true position of sounds on the map, we would like to investigate the bound of sound nodes uniformly distributed on the area. To do that, we place 441 source nodes that need to be localized on grids of 1 m $\times$ 1 m. In order to make the measurements fully pairwise, we assume that a sound emitted by any source node placed within the area can be received by the other nodes. Remark that this network setup is applied to all numerical examples in this section for a fair comparison. Each experimental result described hereafter is the average of 20 trials. Moreover, for a fair comparison, we set a similar constant standard deviation for the standard CRB (5.64 m), which is the average of all above pairwise standard deviations.

Fig. 3 shows the new CRB derived with our proposed TOA model for non-cooperative localization. The CRB

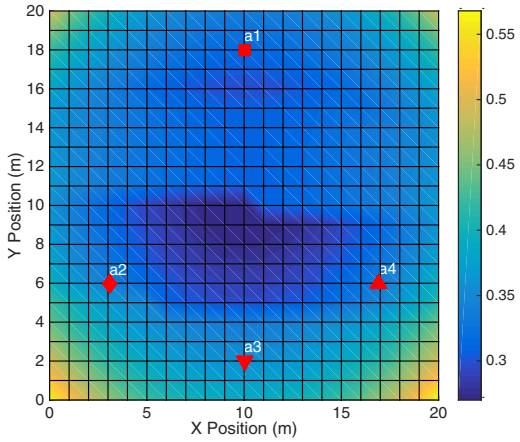

Figure 5. New CRB for TOA cooperative localization with four different kinds of anchors and source nodes. Color bar on the right indicates error bound in meters.

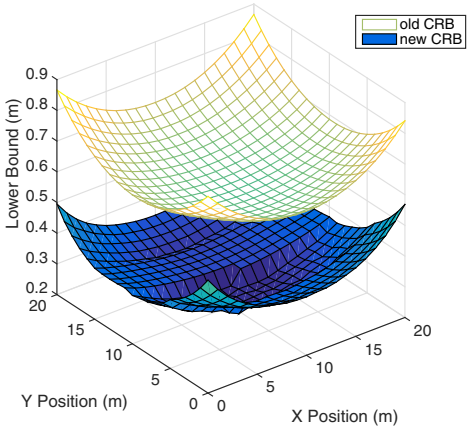

Figure 6. Old CRB vs. new CRB for TOA cooperative localization with the average standard deviation of noises is 5.64 meters.

values vary from about 3.5 meters at the centre to about 7.5 meters at the corners. We noticed that the bound values are high even for the locations near to $a2$ and $a4$, devices with low acoustic latency. Meanwhile, the estimation is quite good for locations near to $a3$ that has very high acoustic latency. This means the error of estimation depends more on the geometric configuration of anchors more than acoustic latency. This is also our intuitive guess. The presence of abundant devices would compensate the acoustic latency since it provides more observations to obtain better estimated values of distribution parameters.

The observation in Fig. 4 shows that both CRBs have a similar shape. However, the new CRB depends more on geometric setup than the old one. The reason is that the old CRB does not fully take geometry into account. That creates similar CRB values for all source nodes. Conversely, the new CRB successfully reflects the geometric effects on localization. The comparison also shows that the new error bound is lower than the old one. This explains why the old bound is limited in integrated geometric impacts, and could be broken by a good location estimator.

Theorem 2: (FIM for Cooperative TOA) All source nodes in S have a shared FIM of which dimension is $2n \times 2n$, denoted by $J_{2n\times 2n}$. Note that J can be written as n^2 block matrices, of which dimension is 2×2.

The elements of diagonal blocks are given by

$$\begin{aligned} J_{2k-1,2k-1} &= \sum_{i\in N_k} \frac{\omega_{ki}\cos^2\alpha_{ki}}{\sigma_{ki}^2}, \\ J_{2k,2k} &= \sum_{i\in N_k} \frac{\omega_{ki}\sin^2\alpha_{ki}}{\sigma_{ki}^2}, \\ J_{2k-1,2k} &= J_{2k,2k-1} = \sum_{i\in N_k} \frac{\omega_{ki}\cos\alpha_{ki}\sin\alpha_{ki}}{\sigma_{ki}^2}. \end{aligned} \tag{19}$$

The elements of non-diagonal blocks, $i \neq k$, if $i \in N_k \bigcap S$:

$$\begin{aligned} J_{2k-1,2i-1} &= J_{2i-1,2k-1} = -\frac{\omega_{ki}\cos^2\alpha_{ki}}{\sigma_{ki}^2}, \\ J_{2k,2i} &= J_{2i,2k} = -\frac{\omega_{ki}\sin^2\alpha_{ki}}{\sigma_{ki}^2}, \\ J_{2k-1,2i} &= J_{2i,2k-1} = J_{2k,2i-1} = J_{2i-1,2k} \\ &= -\frac{\omega_{ki}\cos\alpha_{ki}\sin\alpha_{ki}}{\sigma_{ki}^2}. \end{aligned} \tag{20}$$

Proof: The elements of the diagonal blocks, $k = i$, are derived very similarly the non-cooperative TOA case with regard to all neighbouring nodes, which can be either other source nodes or anchor nodes. Thus the details are omitted for brevity. ■

The CRB for cooperative localization error of the k^{th} node can be described by the sum of the trace of the k^{th} block in the inverse matrix of J

$$E[(\hat{x}_k - x_k)^2 + (\hat{y}_k - y_k)^2] \geqslant J^{-1}_{2k-1,2k-1} + J^{-1}_{2k,2k}. \tag{21}$$

Fig. 5 and 6 show the new CRB and its comparison for cooperative localization using TOA measurements, respectively. Since cooperative localization provides many more observations of the parameters to be estimated, it is possible to achieve much lower error bounds than non-cooperative localization. The error bound has smallest values at positions that are covered by more anchors. That means the accuracy is more affected by the anchor placement than the acoustic latency. The new CRB is also lower than the old one. This observation is consistent with Theorem 2. Consider a similar level of noise for both CRBs, the new CRB is always lower than the old one when $\beta \geq 1$. Furthermore, it is remarkable that the new CRB can show the impacts of the uncertainties even in a cooperative localization manner. In Fig. 6, the

impacts of the uncertainties are represented in the shape of a canal. We observe that once the anchor density increases, the effect tends to fade away and becomes similar to the old CRB [8], [9] with $\omega_{ki} = 1$, but still much lower. This is expected.

B. FIM for TDOA

Since the TDOA model is different from the TOA model, the conditional probability density function (pdf) needs to be rewritten so that the FIM can be derived appropriately, we have

$$f(\delta|\Theta) = \prod_{k\in S} f(\delta|\theta_k) = \prod_{\substack{k\in S \\ i,j\in N_k \\ j>i}} \frac{1}{\sqrt{2\pi}\sigma_{kij}} e^{-\frac{(\delta-d_{kij})^2}{2\sigma_{kij}^2}} \quad (22)$$

where d_{kij} and σ_{kij} are given by Equation 6 and 8, respectively. To derive the FIM, we define $L(\delta|\theta_k) = \log f(\delta|\theta_k)$ as the log-likelihood function for the TDOA measurements

$$\begin{aligned} L(\delta|\theta_k) = &-\log\sqrt{2\pi} \\ &- \frac{1}{2}\log(K_e d_{ki}^{\beta} + K_e d_{kj}^{\beta} + \xi_i^2 + \xi_j^2 + 2\zeta^2) \\ &- \frac{(\delta - d_{kij})^2}{2(K_e d_{ki}^{\beta} + K_e d_{kj}^{\beta} + \xi_i^2 + \xi_j^2 + 2\zeta^2)} \end{aligned} \quad (23)$$

Derivating (23), we obtain the FIM elements for non-cooperative and cooperative localization with TDOA measurements. For brevity, we define the TDOA angles

$$\begin{aligned} \cos\alpha_{kij} &= \cos\alpha_{ki} - \cos\alpha_{kj}, \\ \sin\alpha_{kij} &= \sin\alpha_{ki} - \sin\alpha_{kj}. \end{aligned} \quad (24)$$

Theorem 3: (FIM for Non-cooperative TDOA) Every arbitrary k^{th} source node has its own FIM is $J_{2\times 2}$, of which elements are

$$\begin{aligned} J_{1,1} = \sum_{i\in N_k \bigcap A} \sum_{\substack{j\in N_k \bigcap A \\ j>i}} \Bigg(&\frac{\cos\alpha_{kij}^2}{\sigma_{kij}^2} \\ &+ \frac{\beta^2 K_e^2 (\cos\alpha_{ki} d_{ki}^{\beta-1} + \cos\alpha_{kj} d_{kj}^{\beta-1})^2}{2\sigma_{kij}^4} \Bigg), \end{aligned} \quad (25)$$

$$\begin{aligned} J_{2,2} = \sum_{i\in N_k \bigcap A} \sum_{\substack{j\in N_k \bigcap A \\ j>i}} \Bigg(&\frac{\sin\alpha_{kij}^2}{\sigma_{kij}^2} \\ &+ \frac{\beta^2 K_e^2 (\sin\alpha_{ki} d_{ki}^{\beta-1} + \sin\alpha_{kj} d_{kj}^{\beta-1})^2}{2\sigma_{kij}^4} \Bigg), \end{aligned} \quad (26)$$

$$\begin{aligned} J_{1,2} = J_{2,1} &= \sum_{i\in N_k \bigcap A} \sum_{\substack{j\in N_k \bigcap A \\ j>i}} \Bigg(\frac{\cos\alpha_{kij}\sin\alpha_{kij}}{\sigma_{kij}^2} \\ &+ \frac{\beta^2 K_e^2}{2\sigma_{kij}^4} (\cos\alpha_{ki} d_{ki}^{\beta-1} + \cos\alpha_{kj} d_{kj}^{\beta-1})(\sin\alpha_{ki} d_{ki}^{\beta-1} \\ &+ \sin\alpha_{kj} d_{kj}^{\beta-1}) \Bigg). \end{aligned} \quad (27)$$

Proof: From (23) we define the following two terms

$$U = -\frac{1}{2}\log(K_e d_{ki}^{\beta} + K_e d_{kj}^{\beta} + \xi_i^2 + \xi_j^2 + 2\zeta^2) \quad (28)$$

$$V = -\frac{(\delta - d_{ki})^2}{2(K_e d_{ki}^{\beta} + K_e d_{kj}^{\beta} + \xi_i^2 + \xi_j^2 + 2\zeta^2)} \quad (29)$$

The error bound is

$$E\left[\frac{\partial^2 L(\delta|\theta_k)}{\partial x_k^2}\right] = E\left[\frac{\partial^2 U}{\partial x_k^2}\right] + E\left[\frac{\partial^2 V}{\partial x_k^2}\right].$$

Through steps of partial derivatives, we obtain

$$\begin{aligned} E\left[\frac{\partial^2 L(\delta|\theta_k)}{\partial x_k^2}\right] = &-\frac{\cos\alpha_{kij}^2}{\sigma_{kij}^2} \\ &- \frac{\beta^2 K_e^2 (\cos\alpha_{ki} d_{ki}^{\beta-1} + \cos\alpha_{kj} d_{kj}^{\beta-1})^2}{2\sigma_{kij}^4}. \end{aligned}$$

Analogously, we have other entries of J. ■

Fig. 7 shows that the new CRB for TDOA non-cooperative localization is a bit higher than that of the TOA, which is shown in Fig. 3. However, the error bounds are almost similar in the center. This result is also consistent with Monte Carlo simulations in previous work [15]. The TDOA and TOA non cooperative localization yield roughly the same results, especially in the area bounded by the sensors. In fact, Hahn and Tretter [25] showed that it is possible for TDOA to obtain higher accuracy than TOA when using $|N_k|(|N_k| - 1)/2$ TDOA measurements for all possible anchor pairs instead of using only $(|N_k| - 1)$ TDOAs. We also noticed that the error is more centralized inside the overlapped coverages of anchors in TDOA non-cooperative localization.

Compared with the old CRB in Fig. 8, the new CRB for the TDOA is always lower (noise uncertainties are set equal). The difference is more significant for positions outside of the anchor boundary. Maximum error bound computed by the old CRB is up to 98 m at $(0, 0)^T$ and $(0, 21)^T$. The reason is that the old CRB does not fully exploit the information gained by the TDOA measurements, but the new CRB can.

Theorem 4: (FIM for cooperative TDOA) All source nodes in S have a shared FIM of which dimension is $2n\times 2n$,

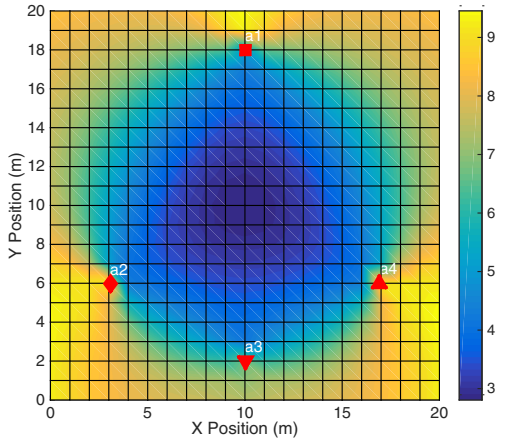

Figure 7. New CRB for TDOA non-cooperative localizationwith four different kinds of anchors and source nodes. Color bar on the right indicates error bound in meters.

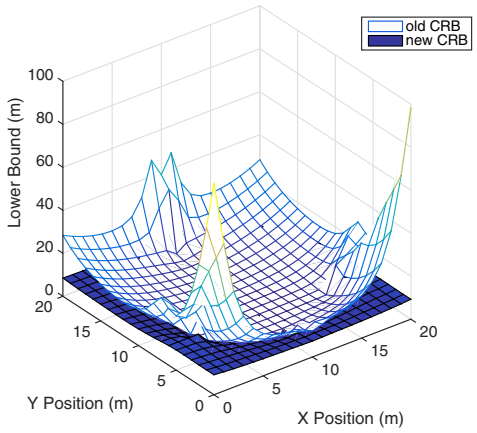

Figure 8. Old CRB vs. new CRB for TDOA non-cooperative localization with the average standard deviation of noises is 5.64 meters.

denoted $J_{2n\times 2n}$.

$$J_{2k-1,2k-1}=\sum_{i\in N_k}\sum_{\substack{j\in N_k\\ j>i}}\left(\frac{\cos\alpha_{kij}^2}{\sigma_{kij}^2}+\frac{\beta^2K_e^2(\cos\alpha_{ki}d_{ki}^{\beta-1}+\cos\alpha_{kj}d_{kj}^{\beta-1})^2}{2\sigma_{kij}^4}\right), \tag{30}$$

$$J_{2k,2k}=\sum_{i\in N_k}\sum_{\substack{j\in N_k\\ j>i}}\left(\frac{\sin\alpha_{kij}^2}{\sigma_{kij}^2}+\frac{\beta^2K_e^2(\sin\alpha_{ki}d_{ki}^{\beta-1}+\sin\alpha_{kj}d_{kj}^{\beta-1})^2}{2\sigma_{kij}^4}\right), \tag{31}$$

$$\begin{aligned}J_{2k-1,2k}&=J_{2k,2k-1}\\&=\sum_{i\in N_k}\sum_{\substack{j\in N_k\\ j>i}}\left(\frac{\cos\alpha_{kij}\sin\alpha_{kij}}{\sigma_{kij}^2}+\frac{\beta^2K_e^2}{2\sigma_{kij}^4}(\cos\alpha_{ki}d_{ki}^{\beta-1}+\cos\alpha_{kj}d_{kj}^{\beta-1})(\sin\alpha_{ki}d_{ki}^{\beta-1}\right.\\&\left.+\sin\alpha_{kj}d_{kj}^{\beta-1})\right).\end{aligned} \tag{32}$$

For non-diagonal elements $i\neq k$, if $i,j\in N_k\bigcap S$ and $j\neq i$,

$$J_{2k-1,2i-1}=J_{2i-1,2k-1}=-\sum_{\substack{j\in N_k\bigcap S\\ j\neq i}}\left(\frac{\cos\alpha_{kij}^2}{\sigma_{kij}^2}+\frac{\beta^2K_e^2(\cos\alpha_{ki}d_{ki}^{\beta-1}+\cos\alpha_{kj}d_{kj}^{\beta-1})^2}{2\sigma_{kij}^4}\right), \tag{33}$$

$$J_{2k,2i}=J_{2i,2k}=-\sum_{\substack{j\in N_k\bigcap S\\ j\neq i}}\left(\frac{\sin\alpha_{kij}^2}{\sigma_{kij}^2}+\frac{\beta^2K_e^2(\sin\alpha_{ki}d_{ki}^{\beta-1}+\sin\alpha_{kj}d_{kj}^{\beta-1})^2}{2\sigma_{kij}^4}\right), \tag{34}$$

$$\begin{aligned}J_{2k-1,2i}&=J_{2i,2k-1}=J_{2k,2i-1}=J_{2i-1,2k}\\&=-\sum_{\substack{j\in N_k\bigcap S\\ j\neq i}}\left(\frac{\cos\alpha_{kij}\sin\alpha_{kij}}{\sigma_{kij}^2}+\frac{\beta^2K_e^2}{2\sigma_{kij}^4}(\cos\alpha_{ki}d_{ki}^{\beta-1}+\cos\alpha_{kj}d_{kj}^{\beta-1})(\sin\alpha_{ki}d_{ki}^{\beta-1}\right.\\&\left.+\sin\alpha_{kj}d_{kj}^{\beta-1})\right).\end{aligned} \tag{35}$$

Proof: The elements of diagonal blocks are derived very similarly to the non-cooperative TDOA case with respect to all neighboring nodes, which may be either source nodes or anchor nodes. Thus the details are omitted for brevity. ■

For TDOA-based cooperative localization, the new CRB is numerically shown in Fig. 9. Because of the ultimately large amount of observations, the new error bound for TDOA-based cooperative localization is significantly lower compared to other approaches. The lowest errors belong to

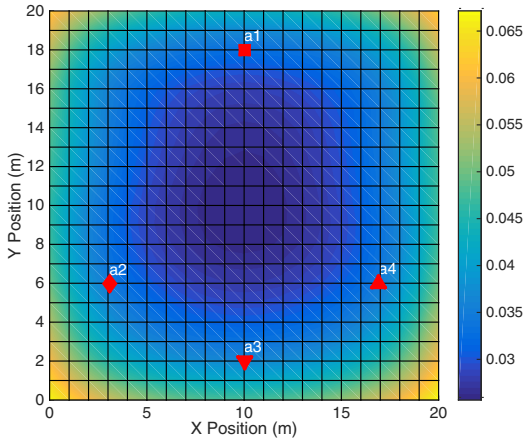

Figure 9. New CRB for TOA cooperative localization with four different kinds of anchors and source nodes. Color bar on the right indicates error bound in meters.

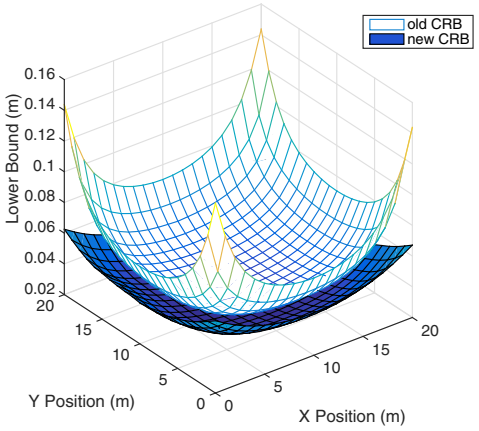

Figure 10. Old CRB vs. new CRB for TDOA cooperative localization with the average standard deviation of noises is 5.64 meters.

the positions at the center. The error increases when the source location moves outwards the anchor ring. Fig. 10 shows the comparison between the new and old CRBs. As it is consistent with Theorem 4, the new CRB is always smaller than the old CRB.

We remark that error bounds for anchored localization in this work are with regard to unbiased estimators. With the advantage of numerous anchors and line-of-sight (LOS) environment in most crowdsensing scenarios, the CRB-based error bounds are valid for most biased estimators too. If the localization problem is significantly biased due to the geometric setup such as inappropriate anchor placement and/or a lot of NLOS environments, it is possible to derive the CRB of biased estimators. However, the bias of the biased estimator needs to be known. Let $b(\theta)$ denote the given bias, the bound is given by

$$E[(\hat{\theta}-\theta)^2] \geqslant \frac{[1+b'(\theta)]}{J}. \tag{36}$$

The bound for any unbiased estimator is a special case of (36) when $b(\theta)=0$.

VII. Conclusion and Future Work

In this paper, we have proposed the new CRBs for anchored localization with regard to diverse non-deterministic noise found in TOA and TDOA measurements. In particular, we developed an Android application and measured the possible noises in the context of crowd monitoring applications developed with Android smartphones. With the new range-based models that include the measured noises, the derivation leads to the new FIM that is different from the former ones. The new bounds for both non-cooperative and cooperative localization categories are theoretically and numerically shown to be better in terms of providing insight into the effects of signal-to-noise ratio, data processing latency, inaccurate time synchronization, and anchor placement. Therefore, the new localization bounds can serve as a tool to aid designing a localization system. The new CRBs also show the potential of sound localization with Android smartphones, albeit finding a good solution of which performance is close to the new bound is challenging.

Acknowledgment

This work is supported by the SenSafety project in the Dutch Commit program, www.sensafety.nl.

References

[1] A. Ens, F. Höflinger, J. Wendeberg, J. Hoppe, R. Zhang, A. Bannoura, L. M. Reindl, and C. Schindelhauer, "Acoustic self-calibrating system for indoor smart phone tracking," *International Journal of Navigation and Observation*, vol. 2015, 2015.

[2] J. Wendeberg, T. Janson, and C. Schindelhauer, "Self-localization based on ambient signals," *Theoretical Computer Science*, vol. 453, pp. 98–109, 2012.

[3] K. Liu, X. Liu, L. Xie, and X. Li, "Towards accurate acoustic localization on a smartphone," in *INFOCOM, 2013 Proceedings IEEE*, April 2013, pp. 495–499.

[4] J. Elson and D. Estrin, "Time synchronization for wireless sensor networks." in *IPDPS*, vol. 1, 2001, p. 186.

[5] H. Wang, L. Yip, K. Yao, and D. Estrin, "Lower bounds of localization uncertainty in sensor networks," in *Acoustics, Speech, and Signal Processing, 2004. Proceedings. (ICASSP '04). IEEE International Conference on*, vol. 3, May 2004, pp. iii–917–20 vol.3.

[6] R. B. Langley, "Dilution of precision," *GPS world*, vol. 10, no. 5, pp. 52–59, 1999.

[7] S. T. Smith, "Covariance, subspace, and intrinsic crame r-rao bounds," *Signal Processing, IEEE Transactions on*, vol. 53, no. 5, pp. 1610–1630, 2005.

[8] N. Patwari, A. O. Hero, M. Perkins, N. S. Correal, and R. J. O'dea, "Relative location estimation in wireless sensor networks," *Signal Processing, IEEE Transactions on*, vol. 51, no. 8, pp. 2137–2148, 2003.

[9] C. Chang and A. Sahai, "Estimation bounds for localization," in *Sensor and Ad Hoc Communications and Networks, 2004. IEEE SECON 2004. 2004 First Annual IEEE Communications Society Conference on*. IEEE, 2004, pp. 415–424.

[10] T. Jia and R. M. Buehrer, "A new cramer-rao lower bound for toa-based localization," in *Military Communications Conference, 2008. MILCOM 2008. IEEE*. IEEE, 2008, pp. 1–5.

[11] J. Huang, P. Wang, and Q. Wan, "Crlbs for wsns localization in nlos environment," *EURASIP Journal on Wireless Communications and Networking*, vol. 2011, no. 1, pp. 1–14, 2011.

[12] N. Patwari and A. Hero, "Signal strength localization bounds in ad hoc and sensor networks when transmit powers are random," in *Sensor Array and Multichannel Processing, 2006. Fourth IEEE Workshop on*. IEEE, 2006, pp. 299–303.

[13] Y. Zhao, Y. Yang, and M. Kyas, "Cramér-rao lower bound analysis for wireless localization systems using priori information," in *Positioning, Navigation and Communication (WPNC), 2014 11th Workshop on*. IEEE, 2014, pp. 1–6.

[14] S. Dulman, P. Havinga, A. Baggio, and K. Langendoen, "Revisiting the cramer-rao bound for localization algorithms," *4th IEEE/ACM DCOSS Work-in-progress paper*, 2008.

[15] R. Kaune, "Accuracy studies for tdoa and toa localization," in *Information Fusion (FUSION), 2012 15th International Conference on*. IEEE, 2012, pp. 408–415.

[16] S. O. Dulman, A. Baggio, P. J. Havinga, and K. G. Langendoen, "A geometrical perspective on localization," in *Proceedings of the first ACM international workshop on Mobile entity localization and tracking in GPS-less environments*. ACM, 2008, pp. 85–90.

[17] A. Savvides, W. Garber, S. Adlakha, R. Moses, and M. B. Srivastava, "On the error characteristics of multihop node localization in ad-hoc sensor networks," in *Information Processing in Sensor Networks*. Springer, 2003, pp. 317–332.

[18] Y. Wang, X. Wang, D. Wang, and D. P. Agrawal, "Range-free localization using expected hop progress in wireless sensor networks," *Parallel and Distributed Systems, IEEE Transactions on*, vol. 20, no. 10, pp. 1540–1552, 2009.

[19] N. Salman, H. K. Maheshwari, A. H. Kemp, and M. Ghogho, "Effects of anchor placement on mean-crb for localization," in *Ad Hoc Networking Workshop (Med-Hoc-Net), 2011 The 10th IFIP Annual Mediterranean*. IEEE, 2011, pp. 115–118.

[20] T. Kunz and B. Tatham, "Localization in wireless sensor networks and anchor placement," *Journal of Sensor and Actuator Networks*, vol. 1, no. 1, pp. 36–58, 2012.

[21] P. Stoica and T. L. Marzetta, "Parameter estimation problems with singular information matrices," *Signal Processing, IEEE Transactions on*, vol. 49, no. 1, pp. 87–90, 2001.

[22] R. L. Moses and R. Patterson, "Self-calibration of sensor networks," in *AeroSense 2002*. International Society for Optics and Photonics, 2002, pp. 108–119.

[23] E. R. Robinson and A. H. Quazi, "Effect of sound-speed profile on differential time-delay estimation," *The Journal of the Acoustical Society of America*, vol. 77, no. 3, pp. 1086–1090, 1985.

[24] N. Patwari, J. N. Ash, S. Kyperountas, A. O. Hero III, R. L. Moses, and N. S. Correal, "Locating the nodes: cooperative localization in wireless sensor networks," *Signal Processing Magazine, IEEE*, vol. 22, no. 4, pp. 54–69, 2005.

[25] W. R. Hahn, S. Tretter *et al.*, "Optimum processing for delay-vector estimation in passive signal arrays," *Information Theory, IEEE Transactions on*, vol. 19, no. 5, pp. 608–614, 1973.